

Pumping Slurries Forming Highly Compactible Cakes

Frank M. Tiller,* Theodore Cleveland, and Rong Lu

University of Houston, Houston, Texas 77204-4792

Highly compactible filter cakes respond to pump pressure in an unexpected manner. At relatively low pressures, the filtrate rate reaches a constant, maximum value and does not increase when the pressure increases. Slurries containing large fragile flocs with high porosity (biosolids, and wastewater sludge) lead to highly compactible sediments and filter cakes. When the local specific flow resistance α increases more rapidly than the local effective pressure p_s ($d\alpha/dp_s > 1$), the region of supercompactibility has been reached. Methods are presented for estimating the magnitude of the pressure at which the rate approaches its limiting value. The interaction of centrifugal and constant-rate pumps with slurries of highly compactible materials is analyzed in this article. Centrifugal pumps should be chosen so that the pump pressure does not fall in the region where the rate is unaffected by pressure. Constant-rate pumps lead to exceedingly high pressures at very short times.

Flow through Compactible Cakes

Solutions of differential equations governing flow through compressible sediments and cakes require constitutive equations relating permeability K , specific flow resistance α , and solidosity ϵ_s (volume fraction of solids) to the effective pressure, p_s . Empirical constitutive equations have generally been in the form of power functions of p_s . We shall use the following equations:

$$(\epsilon_s/\epsilon_{s0})^{1/\beta} = (\alpha/\alpha_0)^{1/n} = (K/K_0)^{-1/\delta} = 1 + p_s/p_s \quad (1)$$

where β , n , δ , and p_a are empirical parameters and ϵ_{s0} , α_0 , and K_0 are values for an unstressed cake. Parameters in eq 1 are subject to

$$\alpha K \epsilon_s = 1, \quad \delta = n + \beta \quad (2)$$

which shows that only two of these parameters are independent. It should be noted that the resistance α and permeability K are not in a reciprocal relation.

The magnitudes of n and δ determine the degree of compactibility and have a large effect on cake behavior under load. When both n and δ are greater than unity, a profound change in behavior takes place, and the matrix of particles forming the cake or sediment is termed highly or supercompactible. Above a relatively low pressure (less than 1 atm for biosolids in urban wastewater systems), increasing pump pressure neither increases the flow rate nor decreases the average cake porosity.

In pressure filtration in the absence of inertial and gravitational effects, p_s and the liquid pressure p_L are related by

$$p_L + p_s = p \quad dp_s + dp_L = 0 \quad (3)$$

where p = applied pressure at the cake surface. The quantities p_L and p_s vary with position and time. With the exception of gravity filtration with a falling head,

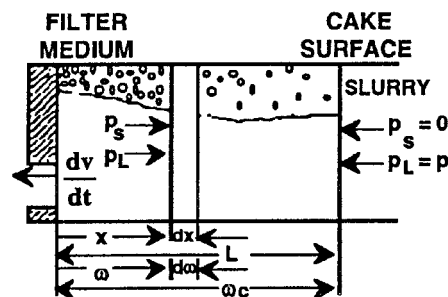


Figure 1. Diagram of a cake with spatial, x , and material, ω , coordinates.

the applied pressure p is either constant or an increasing function of time. For the simplest model usually encountered in the literature, the superficial liquid flow rate q is assumed to be constant throughout the cake and a function of time alone. The solid velocity is assumed to be small in comparison to the liquid velocity and is normally neglected.

Tiller et al.¹ made a study of liquid and solid velocities in cakes being compacted during constant pressure filtration. In general, q could be considered independent of x for dilute slurries and for cakes having high porosities. As the porosity ϵ_L of cakes decreases as the medium is approached, the local velocity u_L increases. The product $\epsilon_L u_L$ which equals q has a considerably smaller variation than either ϵ_L or u_L .

Darcy's law relates the pressure gradient to the flow rate in the form

$$q = \frac{K}{\mu} \frac{dp_L}{dx} = \frac{1}{\mu \alpha} \frac{dp_L}{d\omega} \quad (4)$$

where q = liquid flow rate/unit area, μ = viscosity, x = distance from the supporting medium to an arbitrary point in the cake, and ω = volume of inert solids/unit area in distance x as illustrated in Figure 1. Permeability is employed in the spatial coordinate system with x , and specific resistance is used with the moving material coordinate ω . Shirato et al.² introduced a more general form of Darcy's formula in which the relative velocity was used and u_L was not assumed to be independent of x . In this approximate analysis, q will

* To whom correspondence should be addressed. Chemical Engineering Department, University of Houston, Houston, TX, 77204-4792. Tel.: (713) 743-4322. Fax: (713) 743-4323. E-mail: Ftiller@UH.EDU.

be assumed to be constant at any given instant. As K and α are functions of p_s in accord with eq 1 and are not functions of the liquid pressure, the differential dp_L must be replaced by $-dp_s$ in eq 4 to give

$$\frac{dv}{dt} = q = -\frac{K dp_s}{\mu dx} = -1 \frac{1}{\mu \alpha} \frac{dp_s}{d\omega} \quad (5)$$

where v = the filtrate volume/unit area and t = time. As K and α are functions of p_s , expressions in eq 5 can be integrated to yield q as a function of the pressure drop across the cake.

The differential volume of solids and the total volume of solids/unit area ω_c are related by

$$d\omega = \epsilon_s dx, \quad \omega_c = \int_0^L \epsilon_s dx = \epsilon_{sav} L \quad (6)$$

The volumes per unit area of slurry and filtrate, v , can be related to the volume of cake solids, ω_c , and cake thickness by means of an overall volumetric balance in the following form:

$$\text{slurry vol.} = \text{cake vol.} + \text{filtrate vol.} \quad (7A)$$

$$\frac{\omega_c}{\phi_s} = \frac{\epsilon_{sav} L}{\phi_s} = L + v \quad (7B)$$

where ϕ_s is the volume fraction of solids in the slurry. Solving for v yields

$$v = \left(\frac{\epsilon_{sav}}{\phi_s} - 1 \right) L = \left(\frac{1}{\phi_s} - \frac{1}{\epsilon_{sav}} \right) \omega_c \quad (8)$$

Although ϵ_{sav} varies with the pressure drop through a cake, it is frequently assumed to be constant and equal to the experimental value obtained at the end of a run.

Flow Rate as a Function of Pressure Drop

Equation 5 can be integrated if q is assumed to be independent of x and ω . Limits of integration are

	x	ω	p_L	p_s
medium	0	0	p_1	$p - p_1$
cake surface	L	ω_c	p	0

The liquid pressure at the medium is related to the medium resistance by

$$p_1 = \mu q R_m \quad (9)$$

and $p - p_1 = \Delta p_c$ the pressure drop across the cake. Using the relations provided in eq 1 and integrating leads to

$$\mu q L = \int_0^{\Delta p_c} K dp_s = K_{av} \Delta p_c = K_0 p_0 \left[\frac{(1 + \Delta p_c / p_a)^{1-\delta} - 1}{1 - \delta} \right] \quad (10)$$

$$\mu q \omega_c = \int_0^{\Delta p_c} \frac{dp_s}{\alpha} = \frac{\Delta p_c}{\alpha_{av}} = \mu \frac{dv}{dt} \omega_c = \frac{p_a}{\alpha_0} \left[\frac{(1 + \Delta p_c / p_a)^{1-n} - 1}{1 - n} \right] \quad (11)$$

Dividing eq 11 by eq 10 provides a useful relationship

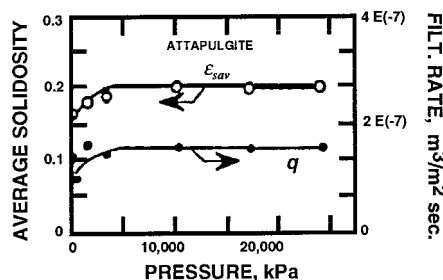


Figure 2. Average solidosity and flow rate as function of the pressure drop during constant pressure filtration.

for the average volume fraction of solids:

$$\frac{\omega_c}{L} = \epsilon_{sav} = \frac{1}{\alpha_{av} K_{av}} = \frac{1}{\alpha_0 K_0} \frac{(1 - \delta)(1 + \Delta p_c / p_a)^{1-n} - 1}{(1 - n)(1 + \Delta p_c / p_a)^{1-\delta} - 1} \quad (12)$$

Equations 10–12 provide relationships between q and ϵ_{sav} and Δp_c for moderately compactible cakes. For highly compactible cakes, n and δ exceed unity, and $(1 - n)$ and $(1 - \delta)$ are negative. Equations 10–12 are best changed into other forms to demonstrate a distinct change in behavior. Equations 11 and 12 become

$$\mu q \omega_c = \frac{p_a}{(n - 1) \alpha_0} \left[1 - \frac{1}{(1 + \Delta p_c / p_a)^{n-1}} \right] \quad (13)$$

$$\epsilon_{sav} = \epsilon_{s0} \frac{(\delta - 1) \left[1 - 1 / (1 + \Delta p_c / p_a)^{n-1} \right]}{(n - 1) \left[1 - 1 / (1 + \Delta p_c / p_a)^{\delta-1} \right]} \quad (14)$$

As the pressure drop increases indefinitely, eqs 13 and 14 approach the following limiting values:

$$\mu q \omega_c = p_a / (n - 1) \alpha_0 \quad (15)$$

$$\epsilon_{sav} = \epsilon_{s0} (\delta - 1) / (n - 1) \quad (16)$$

Both q and ϵ_{sav} rapidly reach limiting values and then are unaffected by further increases in Δp_c . For biosolids encountered in urban wastewaters, the limiting values predicted by eqs 15 and 16 may be reached at less than 0.5 atm. In Figure 2, q and ϵ_{sav} are shown for attapul-gite³ ($\delta = 1.25$, $n = 1.12$, $\beta = 0.13$) as a function of Δp_c up to a maximum filtration pressure of 25370 kPa (3680 psi). In this severe test, the average cake solidosities and flow rates were measured for various constant pressure filtrations. Beginning with $\epsilon_{s0} = 0.09$, ϵ_{sav} rose to 0.2 and remained unchanged. Substitution of the parameters into eq 13 produces $\epsilon_{sav} = 0.19$ which is in reasonable agreement considering the accuracy of the parameters.

Constant Rate Filtration

If the rate is constant, the volume is given by $v = qt$. Substituting this value for v in eq 8 and solving for ω_c produces

$$\omega_c = \frac{\phi_s}{1 - \phi_s / \epsilon_{sav}} qt \quad (17)$$

This equation can be substituted into eqs 11 and 13 respectively for moderately ($n < 1$) compactible cakes. Use of eq 11 leads to

$$\frac{\mu\phi_s}{1 - \phi_s/\epsilon_{sav}} q^2 t = \frac{p_a}{(1-n)\alpha_0} \left[\left(1 + \frac{\Delta p_c}{p_a} \right)^{1-n} - 1 \right] \quad (18)$$

Although ϵ_{sav} changes with Δp_c , the variation of ϕ_s/ϵ_{sav} is small for the frequently encountered case of dilute slurries, and does not have a large effect on the term $(1 - \phi_s/\epsilon_{sav})$. When $\Delta p_c/p_a$ reaches a sufficiently large value, eq 18 can be approximated by

$$\Delta p_c^{1-n} = \frac{(n-1)\alpha_0\mu\phi_s}{(1 - \phi_s/\epsilon_{sav})p_a^n} q^2 t \quad (19)$$

When n exceeds unity, eq 13 is employed and the equation corresponding to eq 19 becomes

$$1 - \frac{1}{(1 + \Delta p_c/p_a)^{n-1}} = \frac{(n-1)\alpha_0\mu\phi_s}{(1 - \phi_s/\epsilon_{sav})p_a} q^2 t \quad (20)$$

It is clear that a substantial change occurs when n becomes greater than unity. Solving for Δp_c in eq 19 and combining the parameters yield

$$\Delta p_c = c_1 (q^2 t)^{1/(1-n)} \quad (21)$$

When $n = 0$ the material is incompressible and Δp_c is linear in t . For $n = 0.5$ and 0.75 , the relationship leads to $(q^2 t)^2$ and $(q^2 t)^4$ and successively higher powers as n approaches unity. The effect of increasing values of n is demonstrated in Figure 3. Relative scales for both pressure and time have been adopted in order to illustrate the profound effect that the compactibility coefficient n exerts on the shape of the curves. For an incompressible cake with $n = 0$ and negligible medium resistance, both the pressure and the cake thickness increase linearly with time. When n equals 0.5 , the exponent in eq 18 equals 2.0 , and the pressure is parabolic in the time. As n increases, the power also increases; when $n = 0.9$, a tenth power results. Although eq 18 is not theoretically correct for $n = 1$, it is clear that an increasingly steep relationship with a vertical asymptote of relative time equal to unity is approached.

Two plots of experimental data for Kaolin⁴ and Fe(OH)₃⁵ along with calculated values for highly compactible activated sludge⁶ with $n = 1.4$ are included in Figure 3. The reference points for the experimental runs were as follows: Kaolin: $t = 100$ min, $p = 496$ kPa (72 psi); Fe(OH)₃: $t = 18$ min, $p = 689$ kPa (100 psi). The experimental curves for the two materials lie in positions predicted by eq 19. Although the calculated values for the activated sludge appear to follow the trends exhibited by the pressure versus time curves for materials with $n < 1$, there are distinct differences which will be considered next.

Supercompactibility and Constant Rate

When $n > 1$, the behavior of filter cakes undergoes a distinct change as illustrated in Figure 3 where the flow rate and average solidosity were unaffected by increasing pressure drop across the cake. Assuming that the pressure drop and time are related by eq 17 when $n > 1$, plots are shown in Figure 4 for the materials whose characteristics are given in Table 1. A flow rate of $q = 0.0001$ m/s, $\mu = 0.001$ Pa·s, and $\phi_s = 0.003$ was chosen for the calculations. At other flow rates, the time scale would be proportioned to the square of q .

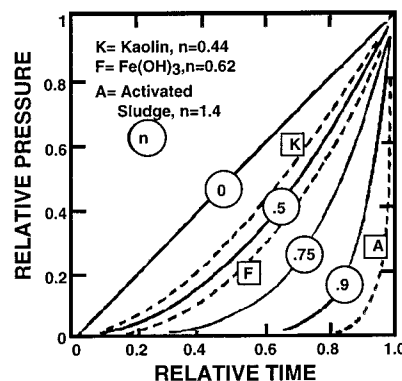


Figure 3. Constant-rate filtration of compactible materials illustrating the effect of n . The curves marked 0.5 , 0.75 , and 0.9 are power functions with powers respectively given by 2 , 4 , and 10 .

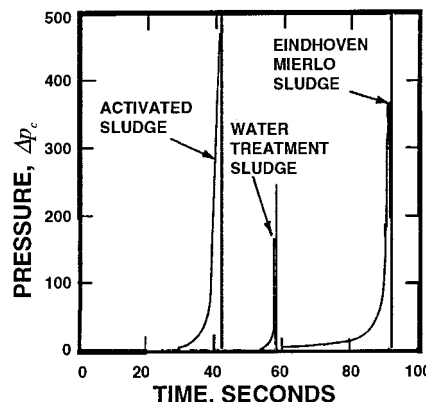


Figure 4. Pressure drop, Δp_c , vs time for supercompactible materials with $n > 1$. Calculations based on eq 22 with $q = 0.0001$ m/s for the activated and Eindhoven–Mierlo sludges, and 0.001 m/s for the water treatment sludge.

Table 1. Parameters for Highly Compactible Materials

material	water treatment sludge	Mierlo biosolid	activated sludge
ϵ_{s0}	0.036	0.03	0.05
α_0, m^{-2}	1.02×10^{11}	4.02×10^{12}	3.62×10^{14}
K_0, m^2	2.73×10^{-10}	8.30×10^{-12}	5.53×10^{-14}
β	0.65	0.47	0.26
n	1.95	1.83	1.40
δ	2.60	2.30	1.66
p_a, Pa	18	1000	190
	Dick and Shin ⁷	LaHeij ⁸	Kwon ⁶

At $q = 1.0 \times 10^{-5}$ m/s, the scale would be multiplied by 100. The general shape of the curves at the various rates would be retained with a sharp upturn occurring at a value dependent on $\Delta p_c/p_a$ and n . The time approaches an asymptotic value¹ which can be obtained by letting Δp_c approach infinity in eq 20. The asymptotic time is given by

$$q^2 t = \frac{(1 - \phi_s/\epsilon_{sav})p_a}{(n-1)\alpha_0\mu\phi_s} \quad (22)$$

If a value of $q^2 t$ larger than that given by eq 22 is substituted into eq 21, a negative value of Δp_c results. Equation 20 is only valid through the range of effective pressure in which the parameters of eq 1 are constant. As p_s increases, cakes reach a compressed state in which α , K , and ϵ_s approach limiting values; the parameters in eq 1 must be modified. As a consequence, the equations which have been derived are not quantita-

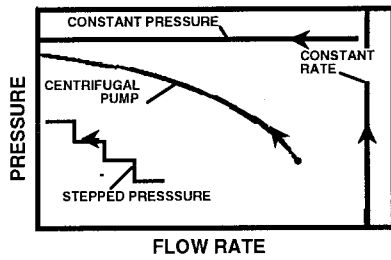


Figure 5. Characteristics related to various mechanisms of pumping. Arrows point in the direction of increasing time.

tively valid at very high pressures. Nevertheless, they provide a reasonable picture of the behavior of highly compactible cakes during pumping.

Although constant-rate pumps have frequently found favor in the filtration industry because of the absence of shear forces which degrade aggregates, the behavior shown in Figures 3 and 4 indicate dangers which may result from sudden increases in pressure. If a recycle line is installed to limit the pressure, operation can continue with a reduction in flow rate. Assuming the pressure drop is sufficiently high for eq 15 to be employed and eq 8 is used to relate ω_c to v , the following equation results:

$$qv = v \frac{dv}{dt} = \frac{1 - \phi_s/\epsilon_{sav}}{\mu\phi_s} \frac{p_a}{(n-1)\alpha_0} \quad (23)$$

Substituting for ϵ_{sav} as obtained from eq 16 and integrating from the time and volume (t_1, v_1) at the end of the constant-rate period to an arbitrary (t, v) leads to

$$v^2 - v_1^2 = \frac{2p_a}{\mu\alpha_0} \left[\frac{1}{(n-1)\phi_s} - \frac{1}{(\delta-1)\epsilon_{s0}} \right] (t - t_1) \quad (24)$$

where $v_1 = qt_1$. Thus, a conventional parabolic filtration follows the constant-rate period.

Comparing eq 23 with eq 11 leads to the following value of the average specific resistance for supercompactible cakes:

$$\alpha_{av} = (n-1)\alpha_0\Delta p_c/p_a \quad (25)$$

Thus, α_{av} is directly proportional to the pressure drop across the cake. When Δp_c is doubled, α_{av} also doubles, and the flow rate is unaffected.

Variable Pressure; Variable Rate Filtration

Variable-pressure, variable-rate operation is frequently encountered because of the extensive use of centrifugal pumps in industry. In the laboratory, stepped pressure experiments can be employed to simulate centrifugal and constant-rate pump operation. Pressure versus flow rate characteristics for various types of pumping mechanisms are illustrated in Figure 5. Arrows point in the direction of increasing time. Although constant pressure operation has dominated the literature and laboratory practice, Avery⁹ stated that the diaphragm and single-screw rotary pumps are the best choices for industry as they do not degrade aggregates and are capable of handling concentrated slurries with high viscosities.

In Figure 6, a characteristic centrifugal pump curve is illustrated with the pressure shown as a function of the rate. As the rate q in the theoretical developments

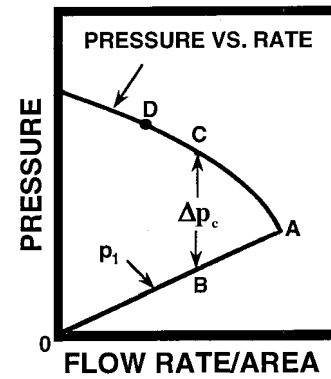


Figure 6. Centrifugal pump characteristics as related to Δp_c .

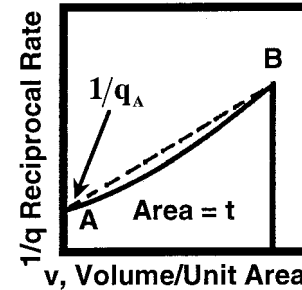


Figure 7. Determination of volume vs time using a centrifugal pump.

is based on unit area, the pump rate supplied by manufacturers must be divided by the filter area. Centrifugal pumps should not be operated at too low a pressure to avoid cavitation. Point A in Figure 6 represents the limiting condition below which the pump should not be operated. The combined resistances of a throttle valve in the feed line and the medium resistance, R_m , supporting the cake lead to a pressure drop, p_1 , represented by the line OA. The throttle is adjusted so that the rate never exceeds the value corresponding to point A. The pressure drop across the cake, Δp_c , is shown by BC and is given by $p - p_1$.

Equation 11 can be adapted to centrifugal pump operation by replacing ω_c by eq 8 and then solving for v , thus,

$$v = \frac{1 - \phi_s/\epsilon_{sav}}{\mu\phi_s} \int_0^{\Delta p_c} \frac{dp_s}{\alpha} = \frac{1 - \phi_s/\epsilon_{sav} p_a (1 + \Delta p_c/p_a)^{1-n} - 1}{\mu\phi_s\alpha_0 q (1-n)} \quad (26)$$

When $n > 1$, eq 13 replaces eq 11. As Δp_c is a function of q , eq 26 leads to v as a function of q . The time required to reach a given point ($q, \Delta p_c$) can be obtained by integrating the expression $dt = dv/q$.

$$t = \int_0^v dv/q \quad (27)$$

The graphical interpretation of eq 27 is given in Figure 7. Starting at point A where filtration begins, $v = 0$ and the rate is given by q_A . The area under the curve in Figure 7 equals the time of filtration. As a rule the curve AB does not vary substantially from linearity, and an upper limit on the time is given by

$$t = \frac{1}{2} \left(\frac{1}{q_A} + \frac{1}{q_B} \right) v \quad (28)$$

For highly compactible cakes, pressures reached on the characteristic curve of Figure 6 may be such that the rate is no longer affected by pressure increases and is controlled by eqs 13 and 15. To develop a criterion for the pressure at which the rate levels off, it will be assumed that the rate q as given by eq 13 has reached a fraction of the maximum rate which is independent of Δp_c and is given by eq 15, then

$$q/q(\max) = 1 - 1/(1 + \Delta p_c/p_d)^{1/(n-1)} = \gamma \quad (29)$$

Solving for Δp_c

$$\Delta p_c = p_a [1/(1 - \gamma)^{1/(n-1)} - 1] \quad (30)$$

If $\gamma = 0.9$, values of Δp_c for the three materials in Table 1 are 15 kPa for Eindhoven Mierlo sludge,⁸ 59.9 kPa for the activated sludge,⁶ and 0.2 kPa for the water treatment sludge.⁷ Although the accuracy of the parameters could be questioned, the results point to the relatively low values at which the flow rate no longer responds to increases in pressure. Pumps should be chosen so that the pressure corresponding to the value obtained from eq 30 lies at a point such as D on Figure 6.

For materials similar to the Eindhoven–Mierlo sludge and Korean-activated sludge, low pressure or vacuum filtration might represent reasonable choices. The low value of 0.2 kPa for the water treatment sludge corresponds to a pressure of about 2 cm of water and points to the use of gravity filtration followed by expression on a belt filter.

Korean-Activated Sludge

The activated sludge investigated by Kwon⁶ of Inje University, Korea, will be used for an example calculation. Adapting eq 10 to materials with $\delta > 1$ leads to

$$\mu qL = \frac{K_0 p_a}{\delta - 1} [1 - 1/(1 + \Delta p_c/p_a)^{\delta-1}] \quad (31)$$

Letting $\mu = 0.001$ Pa·s, substituting values of K_0 , p_a , and δ from Table 1, and using the previously calculated value (eq 30) of $\Delta p_c = 59.9$ kPa produces

$$qL = 1.556 \times 10^{-8} \quad (32)$$

Assuming a cake has a thickness of 1.0 cm leads to $q = 1.556 \times 10^{-6}$ m/s or 0.0023 gpm/sq ft. Pressures above 59.9 kPa would be ineffective, and inclusion of medium resistance would further reduce the calculated rate. A filter with an area of 1000 sq ft (92.9 sq m) would only produce 2.3 gpm (8.71 lit/min) with $L = 0.01$ m. As the thickness increased, the rate would further decrease in accord with eq 32.

The extremely low filtration rate points to the necessity of increasing K_0 and decreasing δ . In practice, inorganic salts (FeCl_3 , $\text{Al}_2(\text{SO}_4)_3$), polyelectrolytes, and filter aids are employed to increase flow rates.¹⁰ In addition to the problem of low rates, the average volume fraction of solids in highly compactible cakes is generally low. Use of eq 14 with $\Delta p_c = 59.9$ kPa leads to a value of $\epsilon_{\text{sav}} = 0.076$. Equation 16 which yields the ultimate limit as Δp_c increases indefinitely yields 0.0825. As the average cake solidosity is frequently below 0.1¹¹ and increasing pump pressure is ineffective, expression

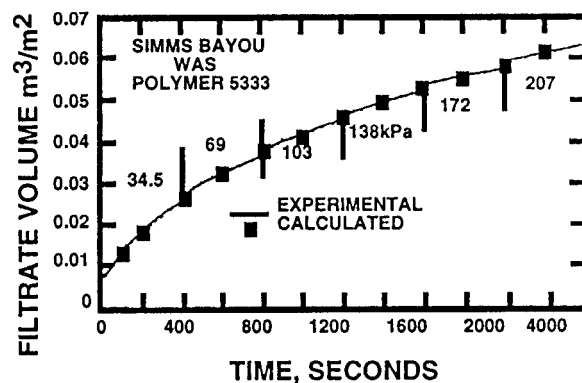


Figure 8. Experimental and calculated values for a waste-activated sludge treated with a cationic acrylamide copolymer.

operations and body forces produced in centrifuges¹² represent options for increasing the percentage of cake solids.

Stepped Pressure Filtration

In general, industrial laboratories are not equipped to perform experiments which yield the parameters appearing in eq 1. An alternative procedure consisting of a series of stepped pressures can be employed to obtain useful information. The most important data relate to identifying the approximate pressure at which q and ϵ_{sav} no longer respond to increasing Δp_c . An example of a stepped pressure experiment is shown in Figure 8. A City of Houston Simms Bayou waste-activated sludge, WAS (3.34 wt % of solids) was treated with differing amounts of cationic acrylamide copolymer in mineral oil. After diluted polymer was mixed with the sludge, the slurry was poured into a filter and pressure was applied with compressed nitrogen. Starting with an initial pressure of 34.5 kPa (5.0 psi), the pressure was increased in increments of 34.5 kPa to a maximum pressure of 206.7 kPa (30 psi) at intervals of 400 s. Except for a slight increase in the slope of v versus t at the end of the first two-step increases (400 and 800 s), the rate of filtrate flow was virtually unaffected by pressures above 34.5 kPa.

Adding the cationic polymer produced substantial improvement in the filterability of WAS. The value of α_0/p_a in eqs 1, 24, and 25 for the treated WAS shown in Figure 8 was approximately one-tenth of the value for the untreated raw sludge. As indicated by eq 24, the filtration volume at a given time is approximately proportional to $(p_a/\alpha_0)^{0.5}$. Thus, the improved value of (α_0/p_a) would result in about a 3-fold increase in volume filtered at a given time.

Equation 24 can be applied to the WAS data of Figure 8, provided the filtration takes place under the condition that the rate depends only on cake thickness and is independent of the pressure. At the start of filtration when time equaled zero, there was 0.0062 m³/m² of filtrate. A severe test of the theory underlying eq 24 consists of using a single point to predict v versus t over the entire pressure range of 34.5–206.7 kPa (5–30 psi) on the basis of a single point. Choosing point A ($t = 1630$ s; $v = 0.06$ m³/m²) leads to

$$v^2 - 0.0062^2 = (2.185 \times 10^{-6})t \quad (33)$$

The squares on Figure 8 represent calculations based on eq 33. Although based on a single point in the 103.7

kPa (25 psi) pressure range, there is only a small difference between the calculated and experimental values over the entire pressure range. Any experimental point in any of the six pressure steps could be employed to predict the entire curve.

Conclusions

The degree of compactibility of filter cakes as reflected in the values of the coefficients n and δ has a significant effect on the relationship of applied pressure to flow rate and percentage of cake solids. When n and δ exceed unity and cakes become supercompactible, a profound change in behavior occurs. As the pressure drop increases, a point is reached at which increasing pressure has a negligible effect on the filtrate flow rate and the percentage of cake solids. Theoretical and experimental methods for identification of the region in which increasing pressure loses its effectiveness have been developed.

Acknowledgment

The authors wish to thank Ronald Clyburn of the City of Houston Wastewater Division for providing samples of the WAS and the cationic polyelectrolyte. Shin Sen (Holly) Chen carried out the stepped pressure filtration experiments.

Nomenclature

c_1 = constant defined in eq 21
 K = local permeability, m^2
 K_0 = unstressed cake permeability, m^2
 K_{av} = average cake permeability, m^2
 L = cake thickness, m
 n = compactibility coefficient eq 1
 p = filtration applied pressure, Pa
 p_a = empirical constant, eq 1, Pa
 p_L = liquid-pressure, Pa
 p_1 = value of p_L , at $x = 0$, Pa
 p_s = effective or compressive pressure, Pa
 Δp_c = liquid-pressure drop across cake, Pa
 q = superficial velocity of liquid, $m^3/m^2 \cdot s$
 q_A, q_B = values of q on Figure 7, $m^3/m^2 \cdot s$
 R_m = medium resistance, m^{-1}
 t = time, s
 v = filtrate volume per unit filter area, m^3/m^2
 x = distance from medium, m
 α = local specific flow resistance, m^{-2}

α_{av} = average specific flow resistance, m^{-2}
 α_0 = unstressed cake specific flow resistance, m^{-2}
 β = compactibility coefficient eq 1
 γ = ratio of q to maximum possible q when $n > 1$
 δ = compactibility coefficient eq 1
 ϵ_s = volume fraction of solids (solidosity)
 ϵ_{sav} = average volume fraction of solids in cake
 ϵ_{s0} = unstressed value of ϵ_s
 μ = liquid viscosity, Pa·s
 ϕ_s = volume fraction of solids in slurry
 ω = volume of inert solids per unit filter area between 0 and x , m^3/m^2
 ω_c = total volume per unit filter area of inert solids in cake, m^3/m^2

Literature Cited

- (1) Tiller, F. M.; Lu, R.; Kwon, J. H.; Lee, D. J. Variable Flow Rate in Compactible Filter Cakes. *Water Res.* **1999**, *13*, 15.
- (2) Shirato, M.; Sambuichi, M.; Kato, H.; Aragaki, T. Internal Flow Mechanism in Filter Cakes. *AIChE J.* **1969**, *15*, 405.
- (3) Tiller, F. M.; Yeh, C. S. Role of Porosity in Filtration, XI, Filtration Followed by Expression. *AIChE J.* **1987**, *33*, 1241.
- (4) Tiller, F. M. Role of Porosity in Filtration, II, Analytical Equations for Constant Rate Filtration, *Chem. Eng. Prog.* **1955**, *51*, 282.
- (5) Tattersfield, G. A Quantitative Study of the Filtration of a Compressible Sludge. M.S. Thesis, Massachusetts Institute of Technology, 1922.
- (6) Kwon, J. H. Effects of Compressibility and Cake Clogging on Sludge Dewatering Characteristics. (in Korean), Ph.D. Dissertation, Seoul National University, Korea, 1995.
- (7) Dick, R. I.; Shin, B. S. Effect of Permeability and Compressibility of Flocculent Suspensions on Thickening. *Prog. Water Technol.* **1975**, *7* (2), 137.
- (8) LaHeij, E. J. *An Analysis of Sludge Filtration and Expression*. D.Eng. Dissertation, Technische Universiteit Eindhoven, Eindhoven, The Netherlands, 1994.
- (9) Avery, L. Batch Filtration. in *AIChE Today Series*; AIChE: New York, 1991; p 58.
- (10) Rushton, A.; Ward, A. S.; Holdich, R. G. *Solid-Liquid Filtration and Separation Technology*; VCH Publishers: New York, 1996; Chapter 5.
- (11) Tiller, F. M.; Kwon, J. H. Role of Porosity in Filtration: XIII, Behavior of Highly Compactible Cakes. *AIChE J.* **1998**, *44*, 2159.
- (12) Tiller, F. M.; Hsyung, N. B. How Does Percent Solids Affect Centrifuge Cakes. *Chem. Eng. Prog.* **1993**, *89*, 20.

Received for review July 20, 1998

Revised manuscript received October 13, 1998

Accepted October 19, 1998

IE980451G